



OPEN

DATA DESCRIPTOR

The Glacier Inventory Dataset of the Qilian Mountains for the Period 2018–2019

Xiang Qin^{1,2}, Renjun Wang^{1,2}, Yushuo Liu¹✉, Jinlong Zhang³ & Xia Li^{4,5}

The Qilian Mountains are located in the arid region of northwestern China and represent a vital ecological functional zone in this area. Glaciers in the Qilian Mountains, as the primary source of freshwater, play a crucial role in regulating the regional water cycle, maintaining ecological balance, and supporting socio-economic activities across the region. Against the backdrop of global warming, glaciers in this region have exhibited a clear trend of retreat. However, the glacier inventory data from China's First and Second National Glacier Inventories are relatively outdated and no longer accurately reflect the current state of glacier changes in the area. This study utilized high-resolution satellite imagery from 2018–2019, including data from the Gaofen series (Gaofen-1, Gaofen-2, and Gaofen-6), Ziyuan-3, and Landsat 8, as primary data sources. Glacier boundaries were delineated through visual interpretation, and relevant attributes were supplemented based on the GLIMS (Global Land Ice Measurements from Space) coding scheme. The final product is the Glacier Inventory Dataset of the Qilian Mountains for the period 2018–2019. The results show that a total of 2797 modern glaciers are distributed across the Qilian Mountains, with a combined area of 1489.53 km². This dataset provides valuable support for studies related to glacier change and associated environmental processes in the Qilian Mountain region.

Background & Summary

The cryosphere, covering approximately 52–55% of the Earth's land surface, is a unique and vital Earth system component comprising all forms of frozen water, including glaciers, snow, permafrost, and sea ice¹. Interactions between the cryosphere and other Earth system spheres significantly influence global energy, water, and carbon-nitrogen balances, thereby exerting profound impacts on weather and climate, the hydrological cycle and water resources, ecosystems, and even human sustainable development^{2–5}. Among the various components of the cryosphere, mountain glaciers and polar ice sheets are the most significant. They are dynamic bodies of ice formed through the accumulation and transformation of snowfall and other forms of solid precipitation^{6–9}. In the arid region of northwestern China, mountain glaciers serve as an irreplaceable freshwater resource, playing a critical role in sustaining the ecological environment and supporting human activities^{10,11}.

Over the past century, the global climate has undergone a pronounced warming trend that is both persistent and intensifying, resulting in widespread and irreversible glacier retreat worldwide, with some regions experiencing complete glacier disappearance^{12–17}. This ongoing glacier retreat not only serves as a direct indicator of global climate change but also represents a critical aspect of its impacts. The reduction and loss of glaciers inevitably affect water resource availability, ecosystem stability, and contribute to global sea-level rise. For regions dependent on glacier runoff, glacier disappearance signifies a diminished freshwater supply, potentially leading to significant challenges in agriculture, drinking water security, and energy production^{18–21}. As a major mountain range in northwestern China, the Qilian Mountains not only constitute a critical part of

¹Qilianshan Observation and Research Station of Cryosphere and Ecologic Environment, State Key Laboratory of Cryospheric Science and Frozen Soil Engineering, Northwest Institute of Eco- Environment and Resources, Chinese Academy of Sciences, Lanzhou, 730000, China. ²University of Chinese Academy of Sciences, Beijing, 100049, China. ³Key Laboratory of Remote Sensing of Gansu Province, Heihe Remote Sensing Experimental Research Station, Northwest Institute of Eco-Environment and Resources, Chinese Academy of Sciences, 730000, Lanzhou, China. ⁴Key Laboratory of Western China's Environmental Systems (Ministry of Education), College of Earth and Environmental Sciences, Lanzhou University, Lanzhou, 730000, China. ⁵Gansu Natural Resources Satellite Application Technology Center, Lanzhou, 730000, China. ✉e-mail: yushuo_liu@lzb.ac.cn

the northeastern margin of the Tibetan Plateau but also serve as an important water source region for inland river basins in Asia^{22,23}. Glaciers in the Qilian Mountains, as the primary freshwater resource of the region, play a vital role in regulating the regional water cycle, maintaining ecological balance, and supporting local socio-economic activities^{24–26}. However, consistent with global changes, glaciers in the Qilian Mountains have also exhibited an accelerated retreat in response to the intensifying global warming^{24,25}. Therefore, obtaining up-to-date and high-precision glacier data for the Qilian Mountains is of great importance for in-depth studies of regional glacier changes, as well as for formulating climate adaptation strategies, ensuring water resource security, and promoting sustainable development. However, the previously conducted First and Second National Glacier Inventories of China^{27,28} are relatively outdated (with data corresponding to approximately 1970 and 2007, respectively) and no longer accurately reflect the current status of glacier changes. Consequently, updating and acquiring new glacier data will provide a more accurate basis for research on regional glacier dynamics.

This study utilized high-resolution satellite imagery from 2018 to 2019, including the Gaofen series (Gaofen-1: GF-1; Gaofen-2: GF-2, and Gaofen-6: GF-6), Ziyuan-3 (ZY-3), and Landsat 8, as primary data sources. Glacier boundaries were delineated through visual interpretation, with relevant attributes refined according to the GLIMS (Global Land Ice Measurements from Space) coding scheme, resulting in the Glacier Inventory Dataset of the Qilian Mountains for 2018–2019. This dataset not only provides intuitive observations of the Qilian Mountains' glaciers through remote sensing techniques but also offers researchers high-precision details on glacier boundaries and area changes. It systematically reveals the spatiotemporal distribution and change trends of glaciers in the Qilian Mountains, thereby facilitating enhanced glacier monitoring and conservation efforts in the region.

Methods

Data and framework. In this Qilian Mountain glacier inventory primarily utilized high-resolution satellite remote sensing images acquired during 2018 and 2019. These high-resolution data are provided by the China Centre for Resources Satellite Data and Application (<https://www.cresda.cn/>) and the Geospatial Data Cloud (<https://www.gscloud.cn/>). The 2018 dataset comprised 18 scenes from the GF-1 satellite, 18 scenes from GF-2 satellite, and 6 scenes from the ZY-3 satellite, mainly covering glaciers within Qinghai Province. The 2019 dataset included 6 scenes from GF-1 satellite, 2 scenes from GF-2 satellite, 8 scenes from GF-6 satellite, and ZY-3 satellite, primarily covering glaciers within Gansu Province. Satellite images with minimal cloud and snow cover—or those in which such cover did not affect glacier boundary identification—were selected. Additionally, Landsat 8 imagery acquired during the period of 2018–2020 was used as reference data. Cloud cover and seasonal snow accumulation directly compromise the accuracy of visual interpretation. To mitigate these interferences, we rigorously screened high-resolution imagery during the data selection phase, retaining only those with cloud coverage below 10% and acquired on clear days during the ablation period, thereby substantially reducing cloud and snow influences at the source. Nevertheless, minor residual interferences remain inevitable. To address this, we adopted the methodology of Muhammad & Thapa^{29,30}, integrating Landsat 8 imagery by applying a cloud probability threshold to mask residual cloudy pixels; concurrently, we computed the Normalized Difference Snow Index (NDSI) and excluded snow-covered pixels; finally, we filled the resulting gaps with contemporaneous cloud- and snow-free Landsat 8 pixels to ensure the reliability of the outcomes. The detailed information of the primary images are presented in supplementary information.

The GDEM V3 digital elevation model (DEM) with a 30 m resolution was used as the data source for glacier attribute extraction. The GDEM V3 dataset Developed jointly by Ministry of Economy, Trade and Industry (METI) and National Aeronautics and Space Administration (NASA) is freely available to the public. On August 5, 2019, NASA and METI jointly released ASTER GDEM V3, which builds upon V2 by adding 360000 new optical stereo pairs, primarily to reduce elevation voids and anomalies over water bodies. GDEM V3 can be downloaded from the Geospatial Data Cloud (<https://www.gscloud.cn/>).

All raster layers were processed using QGIS software. The Qilian Mountains extend approximately 800 km in an east-west direction; therefore, the choice of the projection coordinate system for the vector layer must avoid distortion caused by this longitudinal elongation. Ignoring the characteristics of the projection system could affect the accuracy of glacier area calculations. Therefore, both raster datasets and vector layers were projected using the Asia North Albers Equal Area Conic projection with the WGS-84 ellipsoid. The satellite imagery was first processed through band combination to generate false-color composites that enhance the spectral contrast between snow/ice and other surface features. Subsequently, a high-resolution panchromatic band was fused with the false-color imagery to produce enhanced-resolution false-color images.

In this study, glacier boundaries in the Qilian Mountains were delineated using visual interpretation. Compared to automated or semi-automated methods, visual interpretation is more time-consuming but yields highly reliable glacier boundary data. To mitigate the limitations of visual interpretation—namely, its strong dependence on the interpreter's expertise, experience, and attention, as well as potential subjective discrepancies among interpreters in assessing the same image features, which may reduce classification consistency—the delineation was independently performed by multiple experts with over a decade of glacier inventory experience. Each glacier in the Qilian Mountains was manually outlined, followed by three rounds of cross-validation and independent review, thereby minimizing methodological uncertainty and potential bias to the greatest extent possible. With reference to Landsat 8 imagery and DEM data, the primary image was geometrically corrected, followed by visual interpretation to delineate glacier boundaries. Upon completion of glacier boundary vectorization, cross-verification through visual inspection was conducted. After finalizing revisions, glacier attributes were extracted by integrating with DEM data, the workflow diagram was illustrated in Fig. 1.

Glacier extraction and coding. In this study, glacier boundary information was extracted by vectorizing remote sensing imagery. Common methods for extracting glacier area information from satellite images include

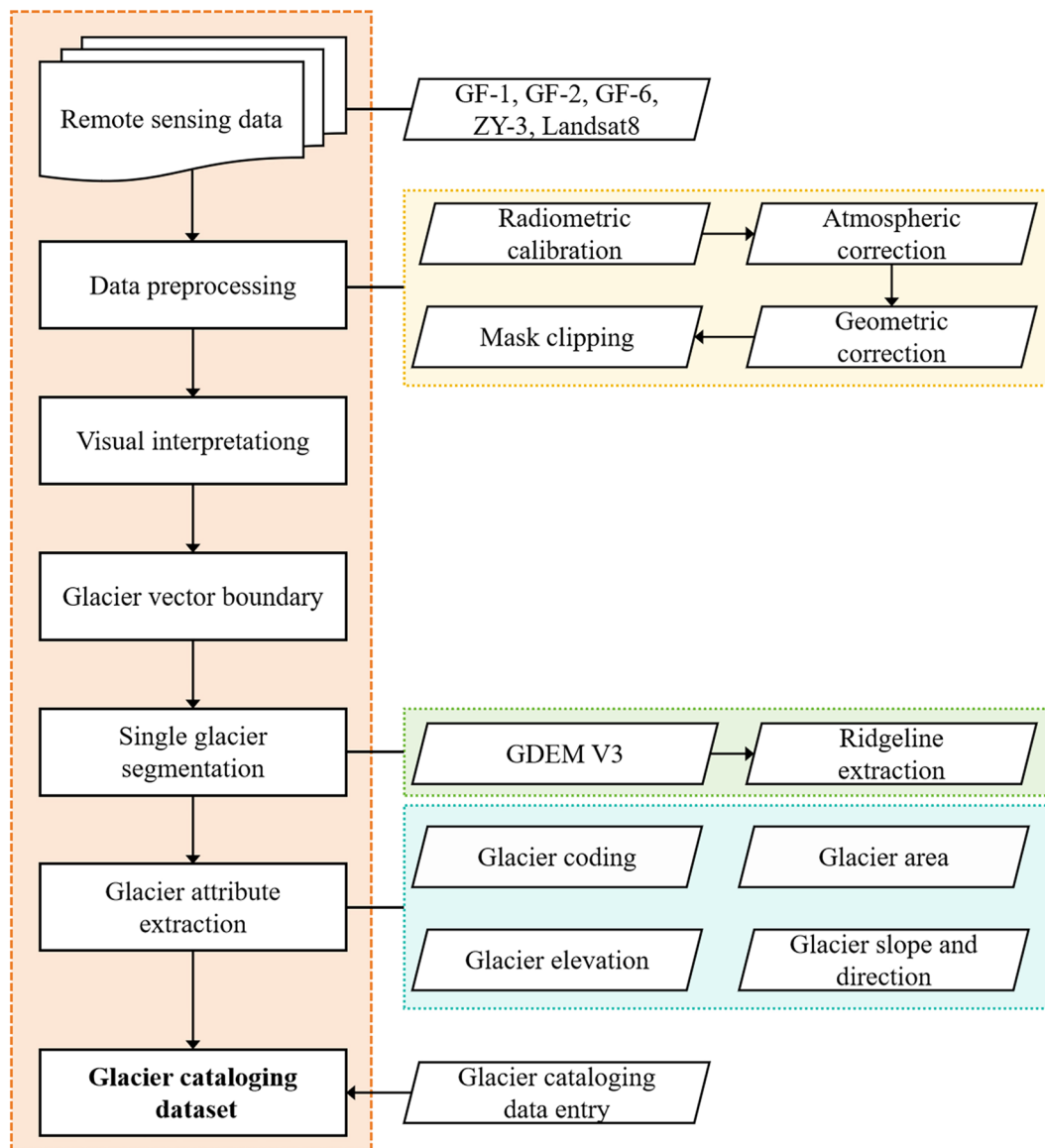


Fig. 1 Workflow for the Production of the 2018–2019 Glacier Inventory Dataset of the Qilian Mountains.

visual interpretation, brightness thresholding, the Normalized Difference Snow Index (NDSI), and supervised classification^{31,32}. Compared to other methods, visual interpretation enables rapid extraction of key features from large volumes of imagery, minimizing reliance on complex data processing. It provides an intuitive representation of information, facilitating quick understanding and decision-making. Therefore, this study employed visual interpretation to process remote sensing images and delineate glacier boundaries.

The First Chinese Glacier Inventory adopted the WGI coding system, which was established in 1977 by the World Glacier Inventory Temporary Technical Service (WGI/TTS) as specified in the “World Glacier Inventory Guidelines”³³. The coding structure consists of the country code (CN for China), the continent code (5 for Asia), the watershed code and the glacier identification number. The watershed code is composed of five digits and characters representing the hierarchy from first- to fifth-order basins. The first-order basin code is denoted by uppercase letters; in the Qilian Mountains, there are two first-order basins with glaciers: the Inland River Basin (Y) and the Yellow River Basin (J). The second- to fourth-order watershed codes are assigned by starting from the outlet of the higher-level watershed and sequentially coding each tributary in a clockwise direction using Arabic numerals. The fifth-order watershed code, representing individual rivers, is denoted by English letters. Glacier identification numbers correspond to the glaciers within the fifth-order watershed, numbered clockwise using Arabic numerals and padded with leading zeros to ensure four digits. In the First Chinese Glacier Inventory, the country code was omitted from the coding scheme.

In the Second Chinese Glacier Inventory, The GLIMS (the Global Land Ice Measurements from Space) identification system was incorporated while retaining the WGI coding scheme. GLIMS identification system assigns a unique identifier to each glacier. The GLIMS code consists of 14 alphanumeric characters include latitude and

Serial Number	Field Name	Data Type	Field Description	Unit	Example
1	FID	Short Integer	Glacier Identification Code	—	1
2	Drng_Code	Text	Watershed Code	—	5J425E
3	FCGI_ID	Text	Glacier Code	—	5J425E0002
4	Image_time	Date	Remote Sensing Image Acquisition Date (format: YYYY-MM-DD)	—	2019-05-03
5	Glc_Area	Double	Glacier Area	m ²	42501.138
6	Glc_Prmt	Double	Glacier Boundary Length	m	7142.85
7	Elv_mean	Double	Glacier Mean Elevation	m	4709.50
8	Elv_median	Double	Glacier Median Elevation	m	4717
9	Elv_min	Double	Glacier Maximum Elevation	m	4582
10	Elv_max	Double	Glacier Minimum Elevation	m	4807
11	Slp_mean	Double	Glacier Mean Slope	degree / °	31.758467
12	Slp_median	Double	Glacier Median Slope	degree / °	29.746744
13	Slp_min	Double	Glacier Minimum Slope	degree / °	9.07515
14	Slp_max	Double	Glacier Maximum Slope	degree / °	52.430187
15	Asp_mean	Double	Glacier Mean Aspect	degree / °	118.359619
16	Asp_median	Double	Glacier Median Aspect	degree / °	21.33139
17	Asp_min	Double	Glacier Minimum Aspect	degree / °	0.296867
18	Asp_max	Double	Glacier Maximum Aspect	degree / °	358.636078

Table 1. Description of the Attribute Fields in the 2018–2019 Qilian Mountains Glacier Inventory Dataset.

longitude of glacier reference point. However, GLIMS lack intuitive representation of glacial geographic location and does not incorporate watershed information. Moreover, for adjacent small glaciers, the codes are highly prone to duplication, thereby compromising the uniqueness of identifiers. Therefore, in this study continues to use the WGI coding method. In cases of omissions or glacier separated, unencoded glaciers are updated only up to the fifth-level watershed code without assigning new glacier identification numbers.

Glacier attribute extraction. Glacier attribute information was extracted utilizing the analytical tools available in the QGIS. The Field Calculator was used to compute geometric parameter of glaciers, such as area and perimeter, retaining three significant digits.

Using DEMs as input, slope gradient and aspect were derived by performing raster terrain analysis tools. Subsequently, the Zonal Statistics tool was used to extract elevation and slop values within each glacier boundary.

Aspect is a circular variable, its mean cannot be directly calculated using zonal statistics. Instead, the extraction of glacier mean aspect followed the method proposed by Davis *et al.*³⁴.

Data Records

The 2018–2019 Qilian Mountains Glacier Inventory Dataset (designated as the Third Glacier Inventory of the Qilian Mountains to distinguish it from the First and Second Inventories) which is stored in Shapefile format is freely available from the National Tibetan Plateau Data Center³⁵.

Data Overview

The attribute table of the Third Glacier Inventory of the Qilian Mountains Dataset comprises 18 fields, including glacier identification codes, remote sensing image acquisition dates, glacier area, perimeter, elevation, slope, and aspect (Table 1). During the cataloging process, glaciers in the eastern section of the Altun Mountains within Gansu Province were also vectorized and their information collected. These glaciers belong to the Danghe and Haerteng Rivers, and to ensure the integrity of the watershed, they were included in the statistical scope of glaciers in the Qilian Mountains. Unless otherwise specified, subsequent analyses will not separately address glaciers in the eastern Altun Mountains section. Within the Qilian Mountains-eastern Altun Mountains region, there are 11 third-level watersheds, which belong to the Hexi inland drainage system, the Qinghai inland drainage system, and the Yellow River drainage system (Table 2).

Technical Validation

Uncertainty assessment. In glacier inventory mapping utilizing remote sensing imagery, the delineation of glacier boundaries constitutes a critical data processing procedure. The precision of glacier boundary interpretation, which benefits from clearly discernible demarcations between glacial and non-glacial areas in the imagery, depends not only on spatial resolution but also on acquisition timing and surface conditions. To quantify the uncertainty U_A in area estimation during feature identification from raster imagery, it is assumed that feature boundaries pass through the center of each pixel. Following co-registration, the area uncertainty U_A of the raster image is calculated using the following equation^{36,37}:

$$U_A = \frac{1}{2} \times l \times \lambda$$

Where l represents the feature perimeter and λ denotes the spatial resolution of the imagery.

River System	Name	Watershed Code	Drainage Area / km ²	Source Mountain Range
Hexi Inland River System	Shiyang River	5Y41	10950	Northern Slope of Lenglong Ridge
	Hei River	5Y42	15490	Northern Slope of Tuolai Nanshan; Southern Mountains of the Corridor
	Beida River	5Y43	9990	Tuolai Mountain; Corridor South Mountains
	Shule River	5Y44	17630	Tuolai South Mountain; Shule South Mountain
	Dang River	5Y45	17050	Shule South Mountain; Danghe South Mountain
Qinghai Inland River System	Buha River (Qinghai Lake)	5Y51	14370	Shule South Mountain; Datong Mountain
	Haerteng River	5Y56	20630	Danghe South Mountain; Northern Slope of Turgen Daban
	Hala Lake	5Y57	4870	Southern Slope of Shule South Mountain; Northern Slope of Haerke Mountain
	Yuka-Tataleng River	5Y58	9890	Southern Slope of Qaidam Mountain; Southern Slope of Turgen Daban
	Bayinguole River	5Y59	5520	Haerke Mountain
Yellow River System	Datong River	5J42	9765	Tuolai Mountain; Northern Slope of Datong Mountain

Table 2. Tertiary Watersheds in the Qilian Mountains and the Eastern Altyn-Tagh Region.

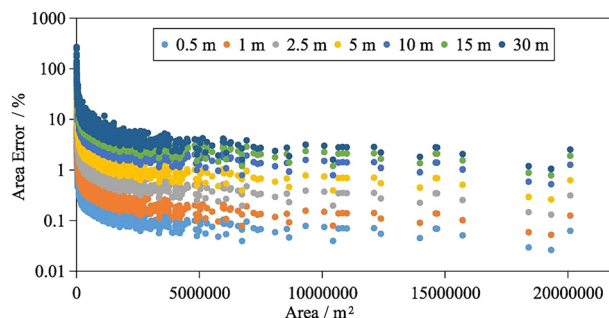


Fig. 2 Glacial area extraction error by raster images with different resolutions.

Using the perimeter attribute from the Qilian Mountains glacier inventory data, we calculated the corresponding area extraction errors for individual glaciers at multiple spatial resolutions commonly found in remote sensing imagery: 0.5 m, 1 m, 2.5 m, 5 m, 10 m, 15 m, and 30 m (Fig. 2). Higher raster image resolution leads to significantly improved accuracy in area identification, while also reducing the minimum detectable target area. Glacier boundaries exhibit irregular shapes, and the uncertainty in glacier area extraction is generally inversely proportional to glacier size, though exceptions exist. For instance, glaciers with similar areas but more circular boundary geometries—characterized by smaller perimeters—demonstrate lower uncertainty. Therefore, to comprehensively evaluate the relationship between glacier dimensions and area extraction uncertainty, the area-to-perimeter ratio (A/P) is adopted as an evaluation metric.

The A/P ratio exhibits an inverse relationship with uncertainty. With an uncertainty threshold set at 0.2 (values below this threshold representing acceptable error margins), the maximum uncertainties in glacier area delineation at raster resolutions of 0.5 m and 1 m remain below this threshold, measuring 0.07 and 0.14 respectively. At coarser resolutions ranging from 2.5 to 30 m, area delineation uncertainties exceed 0.2 when the A/P ratio falls below 5.74, 12.49, 24.96, 37.50, and 49.98 for the respective resolutions. When the uncertainty threshold is set at 0.5, the error constitutes half of the identified feature's area. With raster resolutions of 5 m and above, cases where uncertainty exceeds 0.5 occur, with corresponding A/P ratios falling below 4.82, 9.45, 14.95, and 19.91 respectively. At raster resolutions of 10 m and coarser, the maximum uncertainty in feature area identification exceeds 1.0, indicating that the margin of error is comparable to the area of the feature itself, thus merely meeting the minimum requirement for identification. The corresponding A/P ratios for these resolutions fall below 4.05, 7.06, and 9.45, respectively. In glacier inventory studies, the minimum glacier area has typically been set at 0.01 km²²³⁸. Using 30 m resolution Landsat imagery as an example, this corresponds to approximately 11–12 pixels. However, the associated area extraction uncertainty in such cases already exceeds 0.5.

The aforementioned uncertainty quantification is based on theoretical calculations. In practical area extraction processes, accuracy is also influenced by surface conditions of the features. For instance, the terminus of Laohugou Glacier No. 12 is partially covered by sparse supraglacial debris distributed along the marginal zone, with widths ranging from 14 to 50 m. These widths correspond to 4 and 2 pixels in 15 m and 30 m ground resolution raster images, respectively. In automated glacier boundary identification, factors such as water bodies and cloud cover may cause misinterpretations, while visual interpretation or manual digitization strongly depends on the field experience and subjective judgment of the operator.

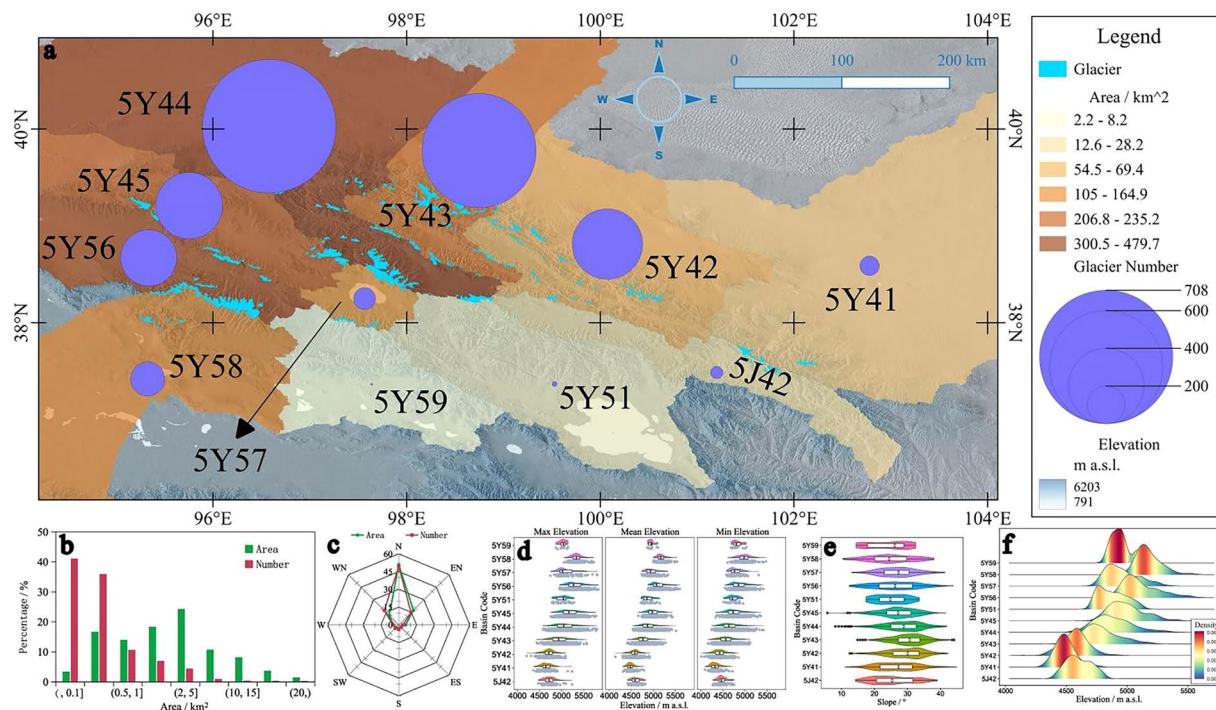


Fig. 3 Spatial distribution of glaciers in the Qilian Mountains (a). Spatial distribution of glacier area and number across tertiary watersheds; (b). Glacier area statistics; (c). Glacier aspect statistics; (d). Distribution of maximum, median, and minimum glacier elevations; (e). Mean glacier slope distribution; (f). Distribution range of mean glacier elevations).

Distribution of glaciers in the Qilian Mountains. In 2018/2019, the Qilian Mountains host a total of 2797 modern glaciers, covering a combined area of 1489.53 km². Among these, the Laohugou Glacier No.12 (code: 5Y448D0012) in the Shule River basin is the only one exceeding 20 km² in size, its area to be 20.09 km². The distribution of glacier numbers and areas in the Qilian Mountains is uneven across different size classes (Fig. 3b,c). As glacier size classes increase, the number of glaciers decreases progressively. The two size categories with the greatest number of glaciers are those smaller than 0.01 km² and between 0.01 to 0.50 km². Glaciers smaller than 0.10 km² dominate in quantity, totaling 1147 glaciers, which accounts for 41.01% of all glaciers in the Qilian Mountains. However, their total area is only 49.03 km², representing just 3.29% of the total glacier area in the region. This area is only twice that of the Laohugou No.12 Glacier (20.09 km²), despite the much larger number of small glaciers. The 0.10 to 0.50 km² size category also contains a considerable number of glaciers, with 1,003 glaciers totaling 247.19 km², accounting for 35.86% of the glacier count and 16.59% of the total glacier area in the Qilian Mountains. Glacier area is more evenly distributed among the size classes of 0.10–0.50 km², 0.50–1.00 km², 1.00–2.00 km², and 2.00–5.00 km², which contribute 16.59%, 13.94%, 18.29%, and 24.22% of the total glacier area, respectively. Among these, the 2.00–5.00 km² category has the largest total glacier area but represents only 4.33% of the total glacier count in the Qilian Mountains.

The largest number of glaciers in the Qilian Mountains face north, accounting for 49.34% of the total glacier count. Glaciers oriented northwest rank second, comprising 17.41%, while those facing west are fewer, representing 4.93%. In terms of area, north-facing glaciers have the greatest cumulative extent, covering 50.83% of the total glacier area in the Qilian Mountains. Glaciers oriented primarily southward are relatively few in both number and area. Southeast-facing glaciers account for the smallest area proportion at 2.63% and represent 2.82% of the total glacier count. The least numerous are southwest-facing glaciers, constituting 3.32% of the glacier count and covering 4.35% of the total glacier area.

There is an overall trend of decreasing glacier size and number from east to west across the Qilian Mountains. Northern slope watersheds exhibit greater glacier area and higher glacier counts than those on the southern slopes (Fig. 3a). The Shule River watershed contains the most extensively developed glaciation in the eastern Qilian–Altun Mountains, accounting for 24.92% of the total number and 31.39% of the total area of glaciers in the region. In contrast, glaciers are sparsely distributed in the Bayinguole, Buha, and Datong River watersheds. Among them, the Bayinguole River watershed has the fewest glaciers, with only 11 glaciers (0.39% of the total), and the smallest total glacier area (0.14%). Although the Buha River is the largest tributary in the Qinghai Lake watershed, only 27 glaciers are present in its upper reaches, accounting for 0.95% of the total glacier number and 0.58% of the total glacier area. The Datong River, an outflow river of the Yellow River watershed and the only one in the Qilian Mountains originating from a glacierized region, hosts 66 glaciers, contributing 2.32% to the total number and 0.88% to the total area of glaciers in the eastern Qilian–Altun Mountains.

The average glacier elevation in the Qilian–Altun Mountains region is 4855.31 m a.s.l., with a general west-to-east decreasing trend. Glaciers on the southern slopes are slightly higher in elevation than those on the

northern slopes (Fig. 3f). The Beida, Shule, and Dang Rivers exhibit a wide range of glacier elevations, corresponding to the large number and total area of glaciers within these watersheds. In contrast, the Shiyang River watershed has the lowest and most concentrated average glacier elevations. The Datong River and Hei River watersheds show similar elevation distribution patterns, while the Yuka–Tataleng River watershed features the highest average glacier elevations, characterized by a relatively symmetric unimodal distribution.

The distribution patterns of maximum, median, and minimum glacier elevations are generally consistent across the watersheds (Fig. 3d). The Beida, Shule, and Dang River watersheds show the widest elevation ranges. The Shiyang River watershed has the lowest maximum, median, and minimum glacier elevations among all watersheds. In terms of maximum elevation, the Shiyang, Hei, and Datong River watersheds exhibit similar values. The Yuka–Tataleng River watershed features the highest glacier elevations across all three metrics (minimum, median, and maximum), with particularly distinct differences in minimum and median elevations compared to other watersheds. The Haerteng River watershed shows a similar maximum elevation distribution to that of the Yuka–Tataleng River watershed.

The distribution of average glacier slopes across watersheds is shown in Fig. 3e. The Beida River watershed has the steepest average glacier slope, reaching 30.44°, while the Shiyang River watershed exhibits the widest range of average slope values. The Bayinguole River watershed has the gentlest average slopes, with a mean of 23.95°. Overall, glacier slopes in the eastern Qilian–Altun Mountains tend to show a west-to-east variation, with slopes generally increasing and then decreasing, which is closely related to glacier morphology and types.

Usage Notes

This dataset has been publicly released and is freely available for download from the National Tibetan Plateau Data Center. When using the data, geographic information software such as ArcGIS, QGIS, or SuperMap can be employed for data reading, editing, and other operations.

Data availability

The peer-reviewed The Glacier Inventory Dataset of the Qilian Mountains for the Period 2018–2019 is publicly available from the National Tibetan Plateau Data Center at <https://doi.org/10.11888/Cryos.tpdc.302479>.

Code availability

The methods used in this study do not involve any automated procedures; therefore, no code is provided with this dataset.

Received: 23 June 2025; Accepted: 31 January 2026;

Published online: 11 February 2026

References

1. Yang, M. *et al.* The Tibetan Plateau cryosphere: Observations and model simulations for current status and recent changes. *Earth-Science Reviews* **190**, 353–369 (2019).
2. Levermann, A. *et al.* Potential climatic transitions with profound impact on Europe: Review of the current state of six ‘tipping elements of the climate system’. *Climatic Change* **110**, 845–878 (2012).
3. Stocker, T. F., Qin, D. & Plattner, G. K. Observations: Cryosphere. *Climate Change 2013: The Physical Science Basis. Contribution of Working Group I to the Fifth Assessment Report of the Intergovernmental Panel on Climate Change* (2013).
4. Qin, D. *et al.* Cryospheric science: research framework and disciplinary system. *National Science Review* **5**(2), 255–268 (2018).
5. Boy, M. *et al.* Interactions between the atmosphere, cryosphere, and ecosystems at northern high latitudes. *Atmospheric Chemistry and Physics* **19**(3), 2015–2061 (2019).
6. Liu, S. *et al.* Changes in the global cryosphere and their impacts: A review and new perspective. *Sciences in Cold and Arid Regions* **12**(6), 343–354 (2021).
7. DeBeer, C. M., Sharp, M. & Schuster-Wallace, C. Glaciers and ice sheets. *World* **215**(705,739), 1565 (2020).
8. Barry, R. G. The cryosphere—past, present, and future: a review of the frozen water resources of the world. *Polar Geography* **34**(4), 219–227 (2011).
9. Muhammad, S. & Thapa, A. Improved MODIS TERRA/AQUA composite Snow and glacier (RGI6.0) data for High Mountain Asia (2002–2018). *PANGAEA* (2019).
10. Su, B. *et al.* Changes in the supply and demand potentials of China’s glacier water resources in the 21st century: Spatiotemporal mismatches and combined effects. *Advances in Climate Change Research* **14**(5), 746–757 (2023).
11. Yao, T. *et al.* The imbalance of the Asian water tower. *Nature Reviews Earth & Environment* **3**(10), 618–632 (2022).
12. Hodge, S. M. *et al.* Climate variations and changes in mass of three glaciers in western North America. *Journal of Climate* **11**(9), 2161–2179 (1998).
13. Baolin, L., Yichi, Z. & Chenghu, Z. Remote sensing detection of glacier changes in Tianshan Mountains for the past 40 years. *Journal of Geographical Sciences* **14**, 296–302 (2004).
14. Owen, L. A. *et al.* Integrated research on mountain glaciers: current status, priorities and future prospects. *Geomorphology* **103**(2), 158–171 (2009).
15. Bolch, T. *et al.* A glacier inventory for the western Nyainqentanglha Range and the Nam Co Basin, Tibet, and glacier changes 1976–2009. *The Cryosphere* **4**(3), 419–433 (2010).
16. Moon, T. Saying goodbye to glaciers. *Science* **356**(6338), 580–581 (2017).
17. Dehecq, A. *et al.* Twenty-first century glacier slowdown driven by mass loss in High Mountain Asia. *Nature Geoscience* **12**(1), 22–27 (2019).
18. Jansson, P. *et al.* The concept of glacier storage: a review. *Journal of Hydrology* **282**(1–4), 116–129 (2003).
19. Sorg, A. *et al.* Climate change impacts on glaciers and runoff in Tien Shan (Central Asia). *Nature Climate Change* **2**(10), 725–731 (2012).
20. Qin, J. *et al.* Assessment of runoff generation capacity and total runoff contribution for different landscapes in alpine and permafrost watershed. *Catena* **249**, 108643 (2025).
21. Qin, Y. *et al.* Snowmelt risk telecouplings for irrigated agriculture. *Nature Climate Change* **12**(11), 1007–1015 (2022).
22. Song, L. *et al.* Changes in characteristics of climate extremes from 1961 to 2017 in Qilian Mountain area, northwestern China. *Environmental Earth Sciences* **81**(6), 177 (2022).

23. Bai, B. *et al.* Changing characteristics of ecosystem and water storage under the background of warming and humidification in the Qilian Mountains, China. *Science of the Total Environment* **893**, 164959 (2023).
24. Sun, M. *et al.* Glacier changes in the Qilian Mountains in the past half-century: Based on the revised First and Second Chinese Glacier Inventory. *Journal of Geographical Sciences* **28**, 206–220 (2018).
25. Zhu, M. *et al.* What induces the spatiotemporal variability of glacier mass balance across the Qilian Mountains. *Climate Dynamics* **59**(11), 3555–3577 (2022).
26. Tian, H., Yang, T. & Liu, Q. Climate change and glacier area shrinkage in the Qilian mountains, China, from 1956 to 2010. *Annals of Glaciology* **55**(66), 187–197 (2014).
27. Wu, L. & Li, X. Dataset of the first glacier inventory in China. *Cold and Arid Regions Science Data Center at Lanzhou* (2004).
28. Guo, W. *et al.* The second Chinese glacier inventory: data, methods and results. *Journal of Glaciology* **61**(226), 357–372 (2015).
29. Muhammad, S. & Thapa, A. An improved Terra–Aqua MODIS snow cover and Randolph Glacier Inventory 6.0 combined product (MOYDGL06*) for high-mountain Asia between 2002 and 2018. *Earth System Science Data* **12**(1), 345–356 (2020).
30. Muhammad, S. & Thapa, A. Daily Terra–Aqua MODIS cloud-free snow and Randolph Glacier Inventory 6.0 combined product (M* D10A1GL06) for high-mountain Asia between 2002 and 2019. *Earth System Science Data* **13**(2), 767–776 (2021).
31. Chu, X. *et al.* Glacier extraction based on high-spatial-resolution remote-sensing images using a deep-learning approach with attention mechanism. *The Cryosphere* **16**(10), 4273–4289 (2022).
32. Rott, H. & Paul, F. Satellite Remote Sensing of Glaciers and Ice Sheets. Glaciers and Ice Sheets in the Climate System: The Karthaus Summer School Lecture Notes 327–348 (2021).
33. Müller, F., Cafilisch, T. & Müller, G. Instructions for compilation and assemblage of data for a World Glacier Inventory. Zurich: Department of Geography, Swiss Federal Institute of Technology (ETH) (1977).
34. Davis, J. C. & Sampson, R. J. *Statistics and data analysis in geology*. New York: Wiley (1986).
35. Liu, Y. Glacier inventory data of Qilian Mountains in 2018/2019. *National Tibetan Plateau / Third Pole Environment Data Center*, <https://doi.org/10.11888/Cryos.tpcdc.302479> (2025).
36. Fujita, K., Sakai, A., Nuimura, T., Yamaguchi, S. & Sharma, R. R. Recent changes in Imja Glacial Lake and its damming moraine in the Nepal Himalaya revealed by *in situ* surveys and multi-temporal ASTER imagery. *Environmental Research Letters* **4**(4), 045205 (2009).
37. Wang, Z. *et al.* Quantitative analysis of Arctic ice flow acceleration with increasing temperature. *Acta Oceanologica Sinica* **40**(1), 22–32 (2021).
38. Paul, F. *et al.* Recommendations for the compilation of glacier inventory data from digital sources. *Annals of Glaciology* **50**(53), 119–126 (2009).

Acknowledgements

This study was supported by the Gansu Province Key Research and Development Program for Ecological Civilization Construction: assessment of Cryospheric Changes and Their Impacts on Water Resources in the Qilian Mountains under the Context of Climate Change (24YFFA010), the Gansu Province Major Science and Technology Project: rapid degradation of the cryosphere and its impact on regional sustainable development (22ZD6FA005), the Project from the second Tibetan Plateau Scientific Expedition and Research Program (STEP) (2019QZKK020103); the 2024 Gansu Provincial Water Resources Baseline Survey Project (2024HTBA02199); Natural Science Foundation of Gansu Province(23JRRA629).

Author contributions

Xiang Qin: Funding acquisition, Supervision, Writing-review& editing; Renjun Wang: Data processing, Data curation, Formal analysis, Writing-original draft; Yushuo Liu: Data processing, Data acquisition, Validation, Writing-review& editing; Jinlong Zhang: Data acquisition, Validation; Xia Li: Data acquisition, Validation.

Competing interests

The authors declare no competing interests.

Additional information

Supplementary information The online version contains supplementary material available at <https://doi.org/10.1038/s41597-026-06782-7>.

Correspondence and requests for materials should be addressed to Y.L.

Reprints and permissions information is available at www.nature.com/reprints.

Publisher's note Springer Nature remains neutral with regard to jurisdictional claims in published maps and institutional affiliations.



Open Access This article is licensed under a Creative Commons Attribution-NonCommercial-NoDerivatives 4.0 International License, which permits any non-commercial use, sharing, distribution and reproduction in any medium or format, as long as you give appropriate credit to the original author(s) and the source, provide a link to the Creative Commons licence, and indicate if you modified the licensed material. You do not have permission under this licence to share adapted material derived from this article or parts of it. The images or other third party material in this article are included in the article's Creative Commons licence, unless indicated otherwise in a credit line to the material. If material is not included in the article's Creative Commons licence and your intended use is not permitted by statutory regulation or exceeds the permitted use, you will need to obtain permission directly from the copyright holder. To view a copy of this licence, visit <http://creativecommons.org/licenses/by-nc-nd/4.0/>.

© The Author(s) 2026